

Preparation of Charged Mosaic Membrane of Sodium Polystyrene Sulfonate and Poly(4-vinyl pyridine) by Conjugate Electrospinning

Yulu Chen,¹ Yimeng Cui,¹ Yuanshan Jia,² Kan Zhan,¹ Hui Zhang,¹ Guoxia Chen,¹ Yadong Yang,¹ Min Wu,¹ Henmei Ni¹

¹School of Chemistry and Chemical Engineering, Southeast University, Southeast University Rd 2, Jiangning, Nanjing 211189, China

²Xi'an Sunward Aerospace Material Co. Ltd., Ba Qiao Zone, Xi'an 710025, China

Correspondence to: H. Ni (E-mail: Henmei_ni@hotmail.com)

ABSTRACT: Conjugate electrospinning of two nozzles with opposite charges was used for the fabrication of charged mosaic membrane (CM membrane). Sodium polystyrene sulfonate (PNaSS) and poly(4-vinyl pyridine) (P4VP) were selected as anionic and cationic exchange elements, respectively. Polyvinyl alcohol was used as the common matrix for the enhancement of mechanical properties by formaldehyde crosslinking. Scanning electron microscope (SEM), transmission electron microscope (TEM), and tensile testing for nanofiber were used for the characterizations of CM membrane. Using the conjugate electrospinning, a simple equation was established to predict the mean diameters of nanofibers. It was proved that the calculated diameters fit well with the experimental data using electrospinning parameters such as concentration of spun solution, collecting speed, rate of solution supply, and distance of two nozzles. TEM picture showed a PNaSS nanofiber was incorporated with a P4VP nanofiber. However, SEM photo indicated that the alignment of composite nanofibers in CM membrane was greatly affected by the concentration of polyelectrolyte. As the concentration of PNaSS increased, the alignment degree decreased. After crosslinking with formaldehyde for 20 h, the tensile strength and Young's modulus of CM membrane reached 11.3 and 24.8 MPa, respectively. The water content and water insolubility of CM membrane were also investigated. © 2014 Wiley Periodicals, Inc. *J. Appl. Polym. Sci.* **2014**, *131*, 40716.

KEYWORDS: electrospinning; fibers; films; kinetics; membranes

Received 16 November 2013; accepted 7 March 2014

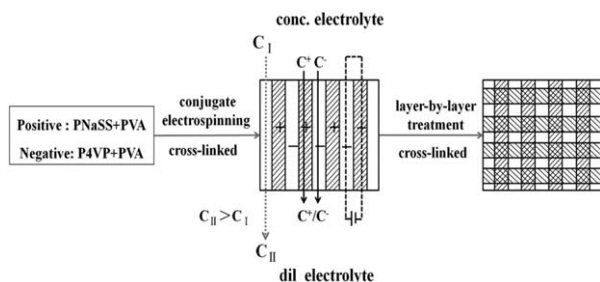
DOI: 10.1002/app.40716

INTRODUCTION

Charge mosaic (CM) membrane made up of alternatively aligned cation- and anion-exchange elements was advantageous to the separation of electrolytes from nonelectrolytes in mixed solutions predicted by Sollner¹ and Kedem and Katchalsky.² It is applicable for the desalination of seawater,³ purification of water,⁴ food additives⁶ and also the biochemical materials,^{7,8} clean energy,^{9,10} and so forth. By far, many approaches have been developed for the preparation of CM membrane.^{11–15} For example, Ni et al.¹¹ used the microspheres for the preparation of CM membrane. The dumbbell-like microspheres of polystyrene/polyvinyl pyrrolidone were prepared. The orientation of polarized dumbbell-like microspheres in the direct current (DC) field created the structure of alternative domains. Takizawa et al. applied the phase growth for the preparation of CM membrane, in which the epitaxial domain were placed on the membrane surface in liquid phase.¹⁴ Fujimoto et al.¹⁵ proposed a method to prepare the CM membrane by the phase separation of sequential (block or graft) copolymers. The phase separation of different components formed the lamellar or cylinder struc-

tures penetrating the block. The epitaxial domain grew gradually to form CM structure. Electrospinning¹⁶ of anionic and cationic polymers were also tried. The layer-by-layer treatment of monolayer nonwovens formed CM membrane. However, many problems are still remained in these approaches. For example, the major problem of phase separation is that the anionic or cationic nanofibers incline to run parallel on the surface, thereby the interruption of domains (element) in the membrane occurs inevitably.¹⁷ In the phase growth method,¹⁸ the condition is crucial but hard to control. As for the layer-by-layer treatment of monolayer nonwovens, the well-defined array of different nanofibers is hard to yield due to the instability of single-needle electrospinning. Moreover, the low strength of the CM membrane is also fatal problem for the application. Therefore, it is necessary to develop a new and facile method to prepare CM membranes with well-defined domains and high mechanical strength.

The nanofiber as one of nanoscale materials can be rationally designed to exhibit novel properties because of their small size, such as the high surface area-to-volume ratio, strong activity, low



Scheme 1. Schematic structure of charged mosaic membrane composed of nanofibers.

porosity, and free assembling in the different nanofilms.^{19–21} Nowadays, electrospinning has been developed as an efficient and low-cost method to fabricate polymer nanofibers. It is a process to control the formation and deposition of polymer nanofibers using an electric field, thereby to produce the electrospun fibers with diameters in the range from several micrometers to nanometer. However, to extend their applications in membrane industry, especially for improving mechanical strength and the structure of nanofibrous mat, many technical problems need to be resolved such as exactly controlled size and well-defined alignment of nanofibers. In the aspect of alignment, reforming the collector setup and loading an additional electric field in collecting device are two prevalent strategies. Fennessey and Farris²² observed that electrospun fibers could be well aligned by changing the plate collector into a drum rotating at high speed. Kim and coworkers²³ designed a collector with two separated pieces of conductive plate, by which the aligned nanofibers were obtained in the gap of collector. Conversely, the control of nanofiber size is dependent on the empirical formulae. For example, Deitzel et al.²⁴ observed the relation of $D = \sqrt{C}$, but Baumgarten²⁵ suggested $D = \sqrt{\eta}$, where D was mean diameter of the nanofiber, C and η were the concentration and viscosity of the polymer solution, respectively. An expanded electro hydrodynamic theory was developed to predict the size of ceramic nanofibers e-spun by a single spinneret.²⁶ It was reported that the maximum difference between predicted value and measured value was less than 30 nm and the ratio between the average difference and the average actual diameter was less than 7%. However, the equation was very complicated. In addition, some terms in the equation were not measurable. For example, the distance and the direction of nanofiber moving in the electric field were unpredictable, because in the mode of single needle, the jet of electrically charged fluid is always pulled by the electrostatic force before it is collected, but disturbed or resisted by the air flow. Due to the resistance of the air and the solvent evaporation, the jet fluid flies randomly.

Li et al.²⁷ invented a new conjugate electrospinning mode. In this mode, two syringes with opposite charge polarity were assigned face to face, by which poly-L-lactic acid and β -tricalcium phosphate (β -TCP) were composited into a continuous nanofiber yarns. Compared with the conventional mode of single needle, this mode is special in several aspects such as the intensity of electric field,²⁸ interaction of positive and negative charges, and jet trajectory. Theoretically, as the opposite electro-

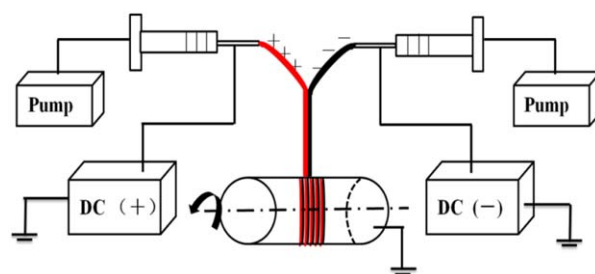
static charges are loaded on the jets spun from the different spinnerets, the jets will attract and finally incorporate with each other while they are flying in the air. As a result, the incorporated jet will lose the charges due to the electric neutralization. At mean time, its speed will be greatly decelerated due to the collision of two fibers; thus, the motion of composited nanofiber in the electric field should be simply dominated by the gravitational force. Such a scenario of nanofiber formation is analogous to the engineering process of common fibers like the melt spinning of polyethylene terephthalate fiber. Therefore, this mode of conjugate spinning provides an engineering feasibility, that is, fabricating the composited nanofiber at first and then controlling the size of nanofiber by adjusting the speed of collecting drum while aligning the nanofibers. For this reason, this mode of conjugate electrospinning was selected to fabricate the CM membrane in this article.

In this article, P4VP and PNaSS were chosen as the cation- and anion-exchange elements, respectively. Because polyvinyl alcohol (PVA) is one of the most popular polymers, which has been used as a membrane matrix,^{29,30} it was selected as the common matrix of both cation- and anion-exchange elements, by which the membrane strength was expected to be improved via facile crosslinking in the postprocessing. At meantime, PNaSS and P4VP are not only environmental friendly due to dissolubility in water but also a promising choice for membrane because of its low cost and relatively high proton conductivity.^{31–33} Utilizing the features of this mode of conjugate electrospinning, in this article, we tried to find the mathematical relationship between the mean size of nanofibers and the various operating parameters such as the solution properties, spinnerets tip distance, and collector speed.

EXPERIMENTAL

Materials

PVA (95% hydrolyzed, average M_w 1750 \pm 50), potassium persulfate (KPS), 2,2'-azobis (isobutyronitrile) (AIBN), formaldehyde, and methanol were purchased from Guoyao, Beijing, China. Sodium styrene sulfonate (NaSS), and 4-vinylpyridine (4VP) were supplied by Aldrich. Methyl iodide (MI) was bought from Xiya, China. All the reagents were used without further treatment, except for 4VP, which was purified by distillation at low pressure. Deionized (DI) water was used for all the experiments, where it was needed.



Scheme 2. Schematic setup of conjugate electrospinning with opposite polarities. [Color figure can be viewed in the online issue, which is available at wileyonlinelibrary.com.]

PNaSS ($M_v = 75,000$) and P4VP ($M_v = 60,000$) were polymerized in the lab by the common free radical polymerization where PNaSS, water and KPS were used as solvent and initiator, respectively. As for P4VP, methanol and AIBN were used as solvent and initiator, respectively. The molecular weight was measured at 25°C by viscometry. For PNaSS, aqueous solution of 0.01M NaCl was used as the medium, while for P4VP, ethanol/H₂O (92/8, w/w) was selected. The corresponding parameters, K and a , are given in the Polymer Handbook.³⁴

Electrospinning

The apparatus of conjugate electrospinning is shown in Scheme 2. Two 5-gauge (0.9 mm outer diameter (OD)), stainless steel needles were installed in opposite sides. Power supply (TE4020EW30-30, Teslaman Co., China) was directly connected to the syringe needles where PNaSS/PVA was positive and P4VP/PVA was negative. Two syringe pumps (RWD202 double two-channel Syringe pump, RWD Life Science Co., China) were used. A self-designed rotating drum (outer diameter, 5 cm) controlled by a stepping motor was used to collect the nanofibers. The voltages of both the negative and positive sides were fixed at 7 kV, and the distance from the tips of two needles to the surface of collector was 15 cm.

Two-layered nanofibrous mat was fabricated by simply changing the direction of the monolayer mat on the collecting drum and then electrospinning once again. The nanofibrous mat was crosslinked by suspending the mat in a chamber full of formaldehyde vapor at 70°C.

Characterization of CM Membrane

The size and alignment degree of composite nanofibers in CM membrane were characterized by the scanning electron microscope (SEM; JSM-6360LV SEM, JOEL Oxford). The samples for SEM observation were prepared as follows: cutting the alumina foil covered with the nanofibrous mat and then sticking it on the stage of SEM. Gold was used as the sputtering material. The number-averaged diameter of nanofiber was a statistic result based on the data of about 200 nanofibers in a SEM image. The alignment degree was also based on the data of about 200 nanofibers. The angle of nanofibers with the largest population in a SEM picture was defined as 0° and then the intersection angles of other nanofibers were determined.

The dispersion of P4VP in the membrane was observed by the transmission electron microscope (TEM; JEM2000EX, TEM, JOEL Oxford) after staining with MI. The samples were prepared as follows: putting a small piece of nanofibrous mat on the water-wetted copper mesh; after drying in a desiccator for 1 day, placing the sample in a 100-mL beaker where two to three droplets of MI was added; and then sealing the beaker with a sheet of plastic film. P4VP was stained for at least 3 days at room temperature until TEM observation. The operation of machines has been reported elsewhere.¹²

Water Content of CM Membrane

The water content of CM membrane was measured according to the reference,³⁵ namely weighing the wet membranes after immersed in DDI water for 48 h.

$$W_c = \frac{W_s - W_d}{(W_s - W_d) + W_d / 1.3}$$

where W_c is the water content; W_s , the wet weights; W_d , the dry weights; 1.0 and 1.3 are the densities of water and PVA, respectively.

Water Insolubility of CM Membrane

The water insolubility of the crosslinked CM membrane was determined by:³²

$$W_i(\%) = \frac{W_2}{W_1} \times 100$$

where W_1 is the weight of dry crosslinked membranes; W_2 , the weight of membrane after immersed in DDI water at 298 K for 1 day and dried at 60°C in vacuum.

Mechanical Strength

The mechanical properties of CM membranes were tested with a gauge length of 50 mm and crosshead speed of 10 mm/min by electronic fiber strength tester (Series IX Automated Materials Testing System, Instron Corporation). Ten samples (20 × 1 mm²) were tested and the mean values were used in the article. All samples were conditioned in a laboratory environment (25°C and relative humidity of 60 ± 3%) for 24 h before testing.

RESULTS AND DISCUSSION

Preparation of Aligned Composite Nanofibrous Mat

As shown in Scheme 1, a simple CM membrane is a well-aligned composite nanofibrous mat, where each nanofiber is a composite of PNaSS and P4VP. Theoretically, the conjugate electrospinning shown in Scheme 2 is an ideal method to prepare such a mat because the two jets with the opposite charges are mutually attractive and finally incorporate into one. Moreover, the charges remained on the half cylindrical surface of composite nanofiber and those on its counterpart are also opposite. It is favorable for the composite nanofibers to alternatively align on the collecting drum. In this article, PNaSS and P4VP were selected as the counter elements of CM membrane. Additionally, to enhance the strength of membrane, PVA was chosen as the common substrate for the formaldehyde crosslinking in the posttreatment of membrane. As we know, the nanofibrous mat of PNaSS and PVA has been prepared by electrospinning.³¹ It was reported that the concentration PNaSS played a key role on the controlling of nanofiber size and its distribution. As the weight ratio of PNaSS was more than 3/7, the nanofiber could not be prepared. The electrospinning of aqueous solution of PNaSS–maleic acid (MA) and PVA was also investigated.³³ It was reported that the mass ratio of PNaSS–MA/PVA should not be larger than 0.4/1, otherwise the preparation of nanofiber would be failed. These references were instructive to our work. Therefore, in this article, the weight ratio of PNaSS/PVA = 1/9 and the concentration of total polymers, 7 wt %, were selected at first for the preparation of composite nanofiber. Conversely, as we know, the aqueous solution of P4VP was not reported to use for the preparation of nanofiber, though the nanofiber of P4VP was successfully prepared using its dimethylformamide (DMF) solution.³² The possible reason

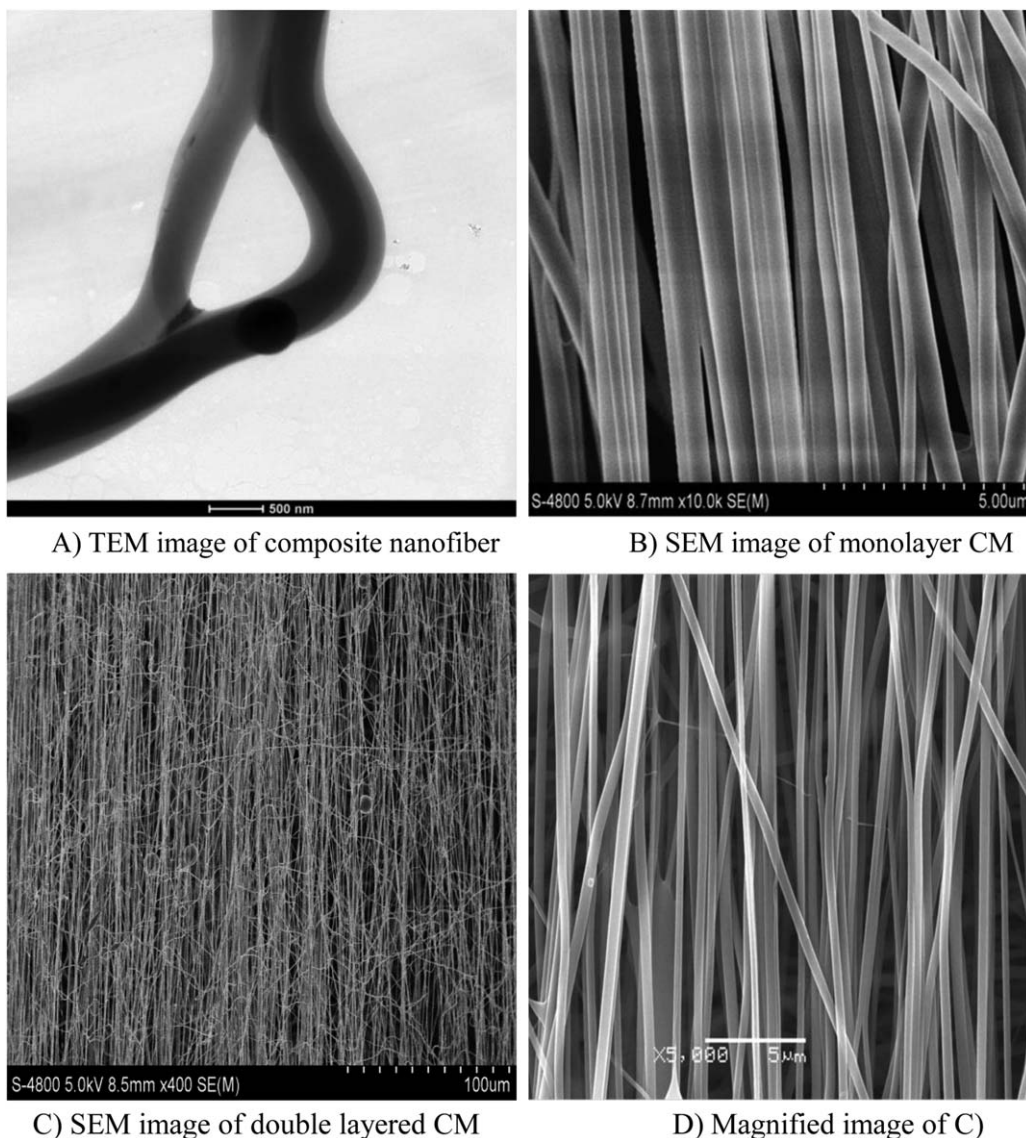


Figure 1. TEM image of PNaSS-P4VP composite nanofiber and SEM image of CM membrane.

was its low solubility in water. However, it was surprisingly observed that P4VP could be well dispersed in the aqueous solution of PVA. The transparent aqueous solution of PVA containing P4VP was readily formulated. This result implies that the concentration of PNaSS was a key factor dominating the process of composite nanofiber formation. Hence, to keep the symmetry of composite nanofiber as much as possible, the weight ratio of P4VP/PVA = 1/9 was selected while the concentration of total polymers was constant at 11 wt %.

Figure 1 shows the TEM image of a composite nanofiber and the SEM image of the CM membrane. As shown in Figure 1(A), the black fiber was P4VP stained by iodinated methane and the white one was PNaSS. It was clear that PNaSS nanofiber was well incorporated with P4VP nanofiber, and also the composite nanofibers were well aligned. Here, we should note that, unfortunately, the TEM image was not obtained, which indicates the structure of alternatively aligned elements of PNaSS and P4VP. The reason was that it was hard to fasten the

composite nanofibrous mat on the copper mesh, the accessory of TEM observation. When water was used as the sticker, the alignment of nanofibers possibly changed. Nevertheless, it is a fact that the alignment of composite nanofibers was severely affected by the concentration of PNaSS.

To further increase the amount of electrolytic polymers, that is, PNaSS and P4VP, in the mosaic membrane, the conjugate electrospinning with high concentration of PNaSS was carried out. However, it was observed that the alignment degree of composite nanofibers was worsened as the concentration of PNaSS increased. As shown in Figure 2, as the concentration of PNaSS increased from 10 to 30%, the distribution of angles was broadened. For example, at 10% PNaSS, there was 58% nanofibers in the oriental angles of 0–10° [Figure 2(A)], whereas at 30%, there was only 46% nanofibers in 0–10° [Figure 2(C)]. As we know, many works have been done to control the alignment of nanofiber, for instance, using the gap of two separated plates²⁶ or the high rotating rate of drum.²⁵ However, in the conjugate

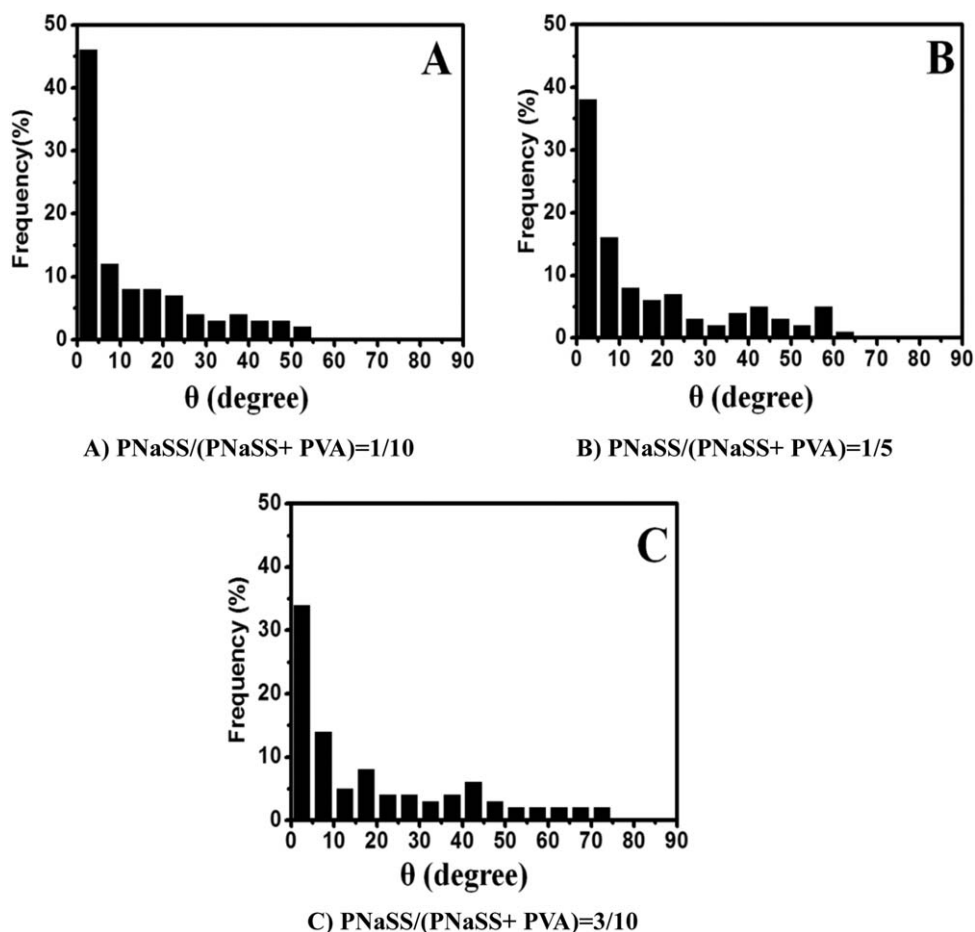


Figure 2. Degree of two aligned nanofibers layers along the axis with different PNASS content.

electrospinning, like the apparatus used in this article (Scheme 2), the factor dominating the alignment of nanofibers was quite different from that in the electrospinning with single nozzle. The two charged jets collided with each other in the air, thus

the momentum of jets played the key role on the motion of composite nanofiber, which finally affected the alignment of nanofibers on the collector. Momentum is determined by the mass and velocity of jets. Because we had no apparatus available

Table I. Parameters Applied for the Calculation of Diameters by Equation

S (cm)	C ₁ (wt %)	ρ ₁ (g/mL)	C ₂ (wt %)	ρ ₂ (g/mL)	V _g (m/s)	V (mL/h)	D _s (μm)	D _c (μm)	n/m
33	6.4	1.02	10.8	1.02	0.41	3	0.28	0.285	1100
33	7.2	1.02	10.8	1.02	0.4	3	0.29	0.295	1100
33	8.4	1.02	10.8	1.02	0.41	3	0.3	0.301	1100
33	7.2	1.02	9.9	1.02	0.42	3	0.28	0.281	1100
33	7.2	1.02	10.8	1.02	0.41	3	0.29	0.292	1100
33	7.2	1.02	12.1	1.02	0.41	3	0.495	0.302	1100
33	7.2	1.02	10.8	1.02	0.17	3	0.46	0.453	1100
33	7.2	1.02	10.8	1.02	0.6	3	0.26	0.241	1100
25	7.2	1.02	10.8	1.02	0.4	3	0.46	0.462	450
40	7.2	1.02	10.8	1.02	0.41	3	0.24	0.242	1600
33	7.2	1.02	10.8	1.02	0.41	5	0.36	0.377	1100
33	7.2	1.02	10.8	1.02	0.41	1	0.2	0.168	1100

Note: S, spinnerets tip distance; C₁ and C₂, concentration of polymers at cathode and anode, respectively; ρ, density of spun solution; V_g, collector speed; V, rate of syringe pump; D_s, SEM diameter; D_c, calculated diameter; n or m, the artificial number of jets applied for the calculation. The density of PVA, 1.27 g/cm³, was used for the calculation instead of the density of polymer in the composite nanofiber.

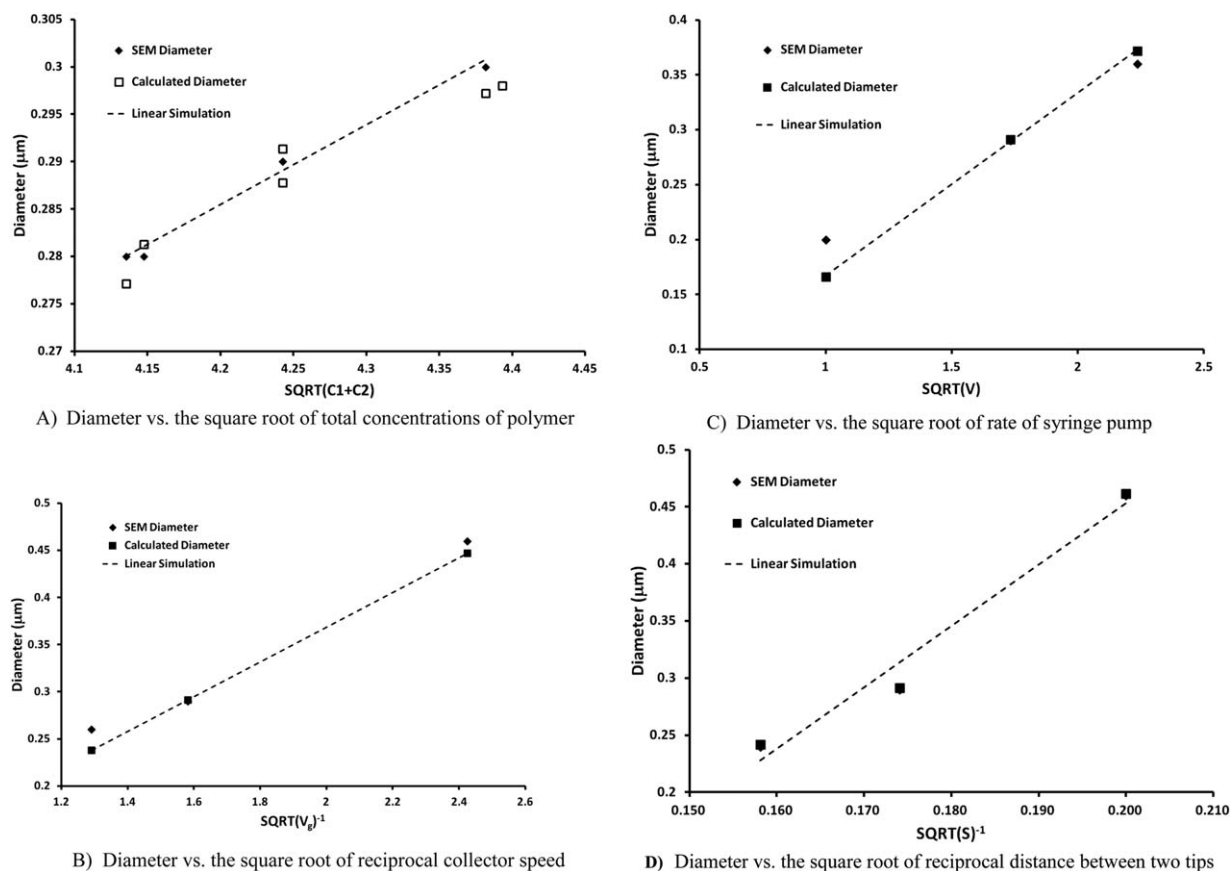


Figure 3. Relationships of SEM diameters of nanofiber with various parameters of electrospinning.

to measure the velocity of jet, it was left as a topic in the future research to find the relationship between the operating parameters and the alignment degree.

Control the Diameter of Nanofiber

It was always a dream to control the diameter of nanofibers in electrospinning. However, so far, only several empirical works have been published. For example, Deitzel et al.²⁴ reported that $D = \sqrt{C}$, and Baumgarten et al.²⁵ suggested that $D = \sqrt{\eta}$, where D was the mean diameter of nanofiber, C and η were the concen-

tration and viscosity of polymer solution, respectively. These works were based on the electrospinning that was equipped with a single spinneret. The charged jets were disturbed by the air flow while they were accelerated in DC field. The instability and unpredictable velocity of jet flight rendered the precise control of diameter to be impossible. In contrast, these defects were not observed in conjugate electrospinning. The jets with opposite charges confined themselves. After incorporating into one fiber, it was free from acceleration force of the DC field due to quenching of charges. These fibers without charges (or little) freely walked in

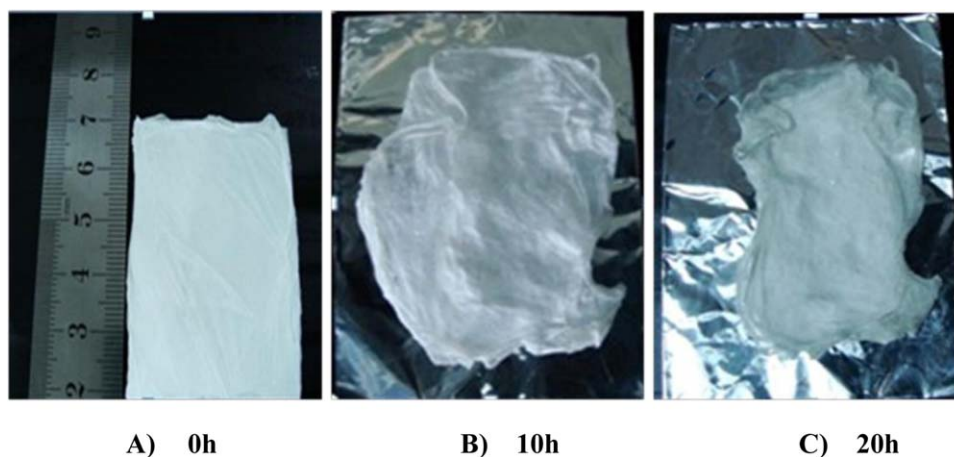


Figure 4. Appearance of PNaSS-P4VP CM membrane against the crosslinking time. [Color figure can be viewed in the online issue, which is available at wileyonlinelibrary.com.]

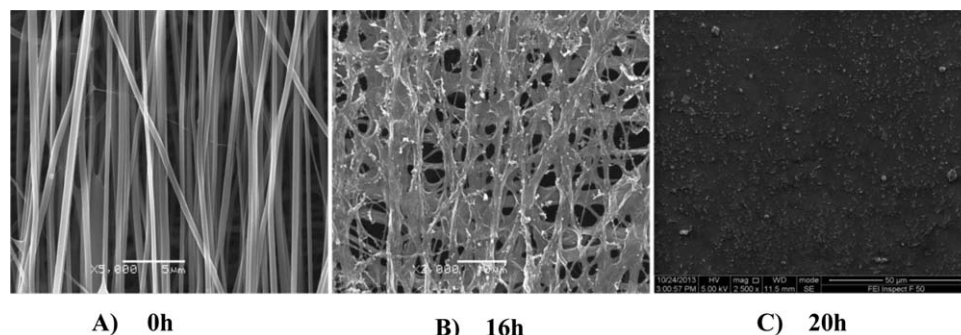


Figure 5. SEM images of PNaSS-P4VP CM membrane at various crosslinking times.

the air, but when they were captured by the collector, their speed was controlled. Therefore, conjugate electrospinning provided a good model to precisely control the diameter of nanofibers.

It should be rational to assume that geometric parameter of the two syringes was equal, the voltage was constant during the fiber formation, the composite nanofiber was an incompressible cylinder, and the effect of gravity on the collecting rate of composite nanofiber was negligible. An equation was obtained readily because the volume of polymers was constant during the process of nanofiber formation.

$$D = \left(\frac{1}{\pi n V_g} \right)^{1/2} \left(\frac{\rho_1 C_1}{\rho_{p1}} \times \frac{V_1}{n} + \frac{\rho_2 C_2}{\rho_{p2}} \times \frac{V_2}{m} \right)^{1/2}$$

where subscripts 1 and 2 represented the terms of cathode and anode, respectively; D , mean diameter of nanofibers (m); ρ , density of spun solution (g/m^3); ρ_p , density of polymer blend (g/m^3); C , the mass concentration of spun solution (%); V , volume rate of syringe pump (ml/s); V_g , speed of collecting (m/s); m and n are the number of jets that the cone of spun solution on the tip of syringe was split into, respectively.

In this equation, only one case was considered: a negative charged jet flow caught a positively charged one. If a charged jet flow was not captured by its counterpart, it would fly to the opposite side. It was true that there were fibers deposited on the syringe in the practice. The other cases, such as that a nega-

tive one captured two or three positively charged ones, were not considered because, we think, the possibility of these cases was low, and more, if the composite jet flow was charged, it should fly to one of the syringes rather than on the collector. Of course, there were the sources of errors. Hence, the equation was transferred into ($n \leq m$),

$$D = \left(\frac{1}{\pi n V_g} \right)^{1/2} \left(\frac{\rho_1 C_1}{\rho_{p1}} V_1 + \frac{\rho_2 C_2}{\rho_{p2}} V_2 \right)^{1/2}$$

As verification of this equation, Table I gives the parameters applied for the calculation and the calculated results as well, while Figure 3 shows the relationship of diameter with the various factors of electrospinning. It is a fact that the jets were dynamically and discontinuously produced. The number of jets produced in a second was undetectable. Therefore, for the calculation, n has to be artificially chosen to fit the measured diameters. However, as shown in Table I, at $n = 1100$, the calculated diameters were fairly closed to SEM diameters, only except for one case that the concentration of spun solution was equal to 12.1%, namely when $C_2 = 12.1\%$, the calculated diameter, 0.302, was quite deviated from the SEM diameter, 0.495. A possible reason was that, as we know, when the concentration of PVA is higher than 10 wt %, the aqueous solution is no longer a real solution, but a gel. In such a case, $n = 410$ was suitable, indicating that the gel was hard to be split. This result supported that the equation was appropriate to predict the

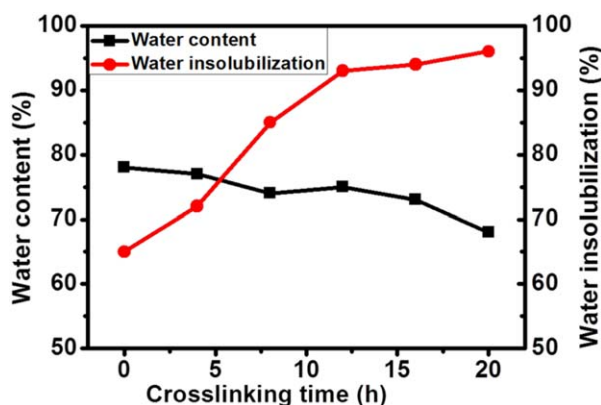


Figure 6. Effect of crosslinking time on the water content and insolubility of PNaSS-P4VP CM membrane. [Color figure can be viewed in the online issue, which is available at wileyonlinelibrary.com.]

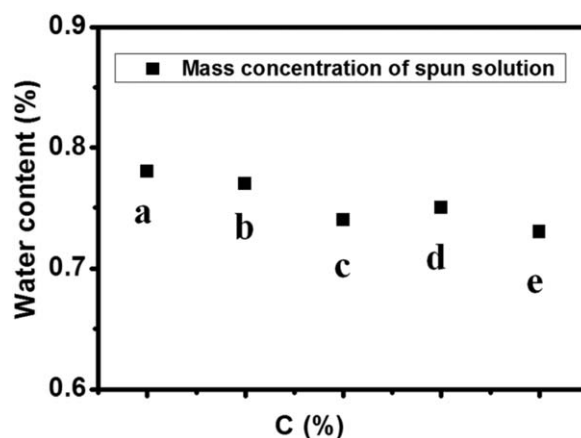


Figure 7. Effect of concentration of spun solution on the water content of PNaSS-P4VP CM membrane.

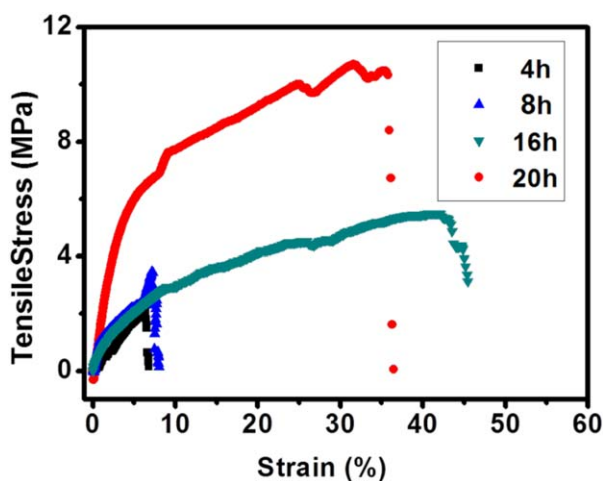


Figure 8. Curves of tensile vs. strain of CM membrane at different crosslinking times. [Color figure can be viewed in the online issue, which is available at wileyonlinelibrary.com.]

diameters of composite nanofibers. Besides, the effect of distance of tow nozzle tips, S , on the diameters was also listed in Table I. As aforementioned, the equation was established under a condition of constant DC field. The strength of DC field varied with the change of S . Hence, S was not included in the equation. However, logically, the effect of S should reflect in the change of n , as the split speed should be determined by the strength of DC field. The shorter S the stronger DC field, thus the larger amount of solution at a moment should be split into jets. As shown in Table I, when S increased from 25, 33 to 40 mm, the SEM diameter decreased from 0.46, 0.29 to 0.24 μm . Correspondingly, if adjusting n from 450, 1100 to 1600, the SEM diameters were well reproduced by calculation. This result indicated that the stronger the DC field, the larger amount of spun solution was split into jets but smaller was the number of jets obtained.

Conversely, to further verify the correctness of equation, the simulation was carried out using various detectable parameters. As shown in Figure 3, the linear relationship was obvious. For example, the SEM diameters were directly proportional to the parameters such as $(C_1 + C_2)^{1/2}$, $V_g^{-1/2}$, $V^{1/2}$, and $S^{-1/2}$. The linear relationship of $D - S^{-1/2}$ should be worthy of comment. It indicated that it was appropriate to use $n^{-1/2}$ to represent the effect of DC field in the equation.

All the above results proved that the equation was applicable for the prediction of nanofiber diameter in the conjugate electrospinning. However, a noticeable fact was that this equation was applicable under the confined conditions, namely that the nanofiber could be prepared without any beads and the collecting speed should be in a proper range matchable with the supply rate of syringe pump.

Waterproof Properties

To improve the waterproof properties and mechanical strength of CM membranes as well, as shown in Scheme 2, the two-layered CM membrane was prepared by orthogonally adjusting the direction of aluminum foil on the collection drum and then

crosslinking by formaldehyde vapor at 70°C. Figure 4 shows the change of membrane during the crosslinking, while Figure 5 shows the SEM photo of CM membrane crosslinked. As shown in Figure 4, the membrane shrank and became thin during the process of crosslinking, while as shown in Figure 5, it is clear that the structure of orthogonal alignment of two-layered nanofibers remained even after exposed in the formaldehyde vapor for 16 h. The water insolubility of such CM membranes was shown in Figure 6 (red dots). As expected, the water insolubility decreased from the original 65 to 96% as the crosslinking time increased. Meanwhile, the water content slightly decreased (Figure 6, black dots).

According to Gregor's model, the matrix in a charged membrane was considered as a network of elastic springs.³⁵ Because "swelling pressure" was caused mainly by the osmotic pressure between the matrix and the aqueous solution, the ion-exchange capacity and degree of crosslinkage decided the water content of the membrane.³⁶ Figure 7 shows the water content varying with the spinning solution concentration and crosslink time. As shown in Figure 7, the water content slightly decreased gradually with the increase of solution concentration, regardless of the positive- or negative-spinning solution. It was normal that the charged functional groups played an important role on the CM membrane swelling. The swelling degree increased with the increase of amount of charged functional groups in CM membrane.

Mechanical Properties

Mechanical properties of CM membranes are shown in Figure 8 and Table II against the crosslinking time. It is clear that as the progress of crosslinking, the tensile strength, Young's modulus and strain at break were improved. This result indicated that the crosslinking reaction not only took place within the inside of nanofiber but also happened in the contact area of two nanofibers. However, as the crosslinking time was longer than 16 h, the strain at break of membranes was worsened. For example, at 20 h of crosslinking time, the strain at break of membrane was 37%, less than 47% at 16 h. It is common that the material becomes brittle when the crosslinking degree is excessive.

As shown in Table II, after crosslinked for 20 h, the tensile strength and modulus of membrane were 11.3 MPa (SD = 3.7) and 24.8 MPa (SD = 4.2), respectively. It was superior compared to some CM membranes reported in the references. For example, Kawatoh et al. reported the modulus of ion-exchange membranes CM-1 enhanced by polyvinyl chloride (PVC) was about 19 MPa.³⁷ Higa et al. fabricated the charge mosaic membranes with semi-interpenetrating

Table II. Mechanical Properties of CM Membrane at Different Crosslinking Time

Crosslinking time (h)	Tensile stress (MPa)	Modulus (MPa)	Strain (%)	Thickness (mm)
4	2.1	4.3	7	0.011
8	3.2	8.5	9	0.008
16	4.6	13.2	47	0.006
20	11.3	24.8	37	0.005

network structures by polymer blend.³³ It was reported that the modulus of CM membrane was about 16 MPa after crosslinked with glutaraldehyde.

CONCLUSIONS

CM membrane of PNaSS and P4VP was first successfully fabricated by conjugated electrospinning. The texture structure of CM membrane was characterized by SEM and TEM. It was observed that the composite nanofiber of PNaSS and P4VP was composed of one PNaSS nanofiber and one P4VP nanofiber. However, the alignment of composite nanofibers was greatly affected by the concentration of polyelectrolyte. As the concentration of PNaSS increased, the alignment of composite nanofibers decreased. Using the specialties of conjugate electrospinning described in this article, the mean diameter of composite nanofibers was precisely predictable by an equation, $D = (1/\pi n V_g)^{1/2} \times ((\rho_1 C_1/\rho_{p1})V_1 + (\rho_2 C_2/\rho_{p2})V_2)^{1/2}$. The simulation indicated that SEM diameters were directly proportional to the electrospinning parameters such as $(C_1 + C_2)^{1/2}$, $V_g^{-1/2}$, $V^{1/2}$, and $S^{-1/2}$.

By the layer-by-layer treatment and crosslinking by formaldehyde vapor, the mechanical, water content, and water insolubility of CM membrane were all significantly improved. When the two-layered CM membrane was exposed in formaldehyde vapor for 20 h, the tensile strength and Young's modulus of membrane attained 11.3 and 24.8 MPa, respectively. These results indicated that the crosslinking reaction of PVA not only occurred in composite nanofiber but also took place in the contact area of two nanofibers.

ACKNOWLEDGMENTS

This research was supported by Chinese National Fund for Science (NSFC, 51073035) and the International Corporation Project (201101088) with Science and Technology Bureau, Nanjing Municipal.

REFERENCES

- Sollner, K. *Biochem.* **1932**, *244*, 370.
- Kedem, O.; Katchalsky, A. *Trans. Faraday Soc.* **1963**, *59*, 1918.
- Fukutomi, T.; Takizawa, M.; Nakamura, M. *J. Polym. Sci. Part A: Polym. Chem.* **2003**, *41*, 1251.
- Miyaki, Y.; Nagamatsu, H.; Iwata, M.; Fujimoto, T. *Macromolecules* **1984**, *17*, 2231.
- Rozendal, R.; Sleutels, T.; Hamelers, H.; Buisman, C.; *Water Sci. Technol.* **2008**, *57*, 1757.
- Liang, L.; Ying, S.; *J. Polym. Sci. Part B: Polym. Phys.* **1993**, *31*, 1075.
- Neihof, R.; Sollner, K.; *J. Gen. Physiol.* **1955**, *38*, 613.
- Kumar, A.; Jose, R.; Fujihara, K.; Wang, J.; Ramakrishna, S. *Chem. Mater.* **2007**, *19*, 6536.
- Ramakrishna, S.; Jose, R.; Archana, P.; Nair, A.; Balamurugan, R.; Venugopal, J.; Teo, W. *J. Mater. Sci.* **2010**, *45*, 6283.
- Ni, H.M.; Kamimura, W.; Uchida, M. *Inhal. Toxicol.* **2007**, *19* (Suppl 1), 251.
- Ni, H.M.; Ma, G.; Nagai, M.; Omi, S. *J. Appl. Polym. Sci.* **2000**, *76*, 1731.
- Ni, H.M.; Ma, G.; Nagai, M.; Omi, S. *J. Appl. Polym. Sci.* **2001**, *80*, 2002.
- Homaeigohar, S.; Koll, J.; Lilleodden, E.T.; Elbahri, M. *Sep. Sci. Technol.* **2012**, *98*, 456.
- Takizawa, M.; Sugito, Y.; Oguma, N.; Nakamura, M.; Horiguchi, S.; Fukutomi, T. *J. Polym. Sci. A: Polym. Chem.* **2003**, *41*, 1251.
- Fujimoto, T.; Ohkoshi, K.; Miyaki, Y.; Nagasawa, M.; *Science*, **1984**, *224*, 74.
- Chung, J. B.; DeRocher, J. P.; Cussler, E. *J. Membr. Sci.* **2005**, *256*, 1.
- Molau, G.; *Polymers.* **1970**, *238*, 493.
- Yamauchi, A.; *Int. J. Chem. Eng.* **2012**, *10*, 417179.
- Sun, F.; Yao, C. *J. Text. I.* **2011**, *102*, 633.
- Huang, Z. M.; Zhang, Y. Z.; Kotaki, M.; Ramakrishna, S. *Compos. Sci. Technol.* **2003**, *63*, 2223.
- Reneker, D. H.; Chun, I. *Nanotechnology* **1996**, *7*, 216.
- Fennessey, S. F.; Farris, R. *J. Polymer.* **2004**, *45*, 4217.
- Zong, X.; Kim, K.; Fang, D.; Ran, S.; Hsiao, B. S.; Chu, B. *Polymer.* **2002**, *43*, 4403.
- Deitzel, J.; Kleinmeyer, J.; Hirvonen, J.; Beck, Tan. N. *Polymer.* **2001**, *42*, 8163.
- Baumgarten, P. K. *J. Colloid Interface Sci.* **1971**, *36*, 71.
- Sigmund, W.; Yuh, J.; Park, H.; Maneeratana, V. *J. Am. Ceram. Soc.* **2006**, *89*, 395.
- Li, X.; Yao, C.; Sun, F.; Song, T.; Li, Y.; Pu, Y. *J. Polym. Sci.* **2008**, *107*, 3756.
- Li, M.; He, Y.; Xin, C. *Appl. Phys. Lett.* **2008**, *92*, 213114.
- Duan, B.; Yuan, X.; Zhu, Y. *Eur. Polym. J.* **2006**, *42*, 2013.
- Pan, H.; Li, L.; Hu, L.; Cui, X. *Polymer.* **2006**, *47*, 4901.
- Martwiset, S.; Jaroensuk, K. *J. Polym. Sci.* **2012**, *124*, 2594.
- Song, Y.; Zhan, N.; Yu, M. *Chem. Res. Chin. Univ.* **2008**, *24*, 722.
- Higa, M.; Kobayashi, M.; Kakihana, Y.; Jikihara, A.; Fujiwara, N. *J. Membr. Sci.* **2012**, *10*, 034.
- Brandrup, J.; Immergut, E. H.; Grulke, E. A. *Polymer Handbook*, 4th ed., Wiley, **2003**.
- Helferich, F. *Ion Exchange*, Dover Publications, New York, **1995**; Chapter 5.1, pp 96–97.
- Andrii, Y. *Desalination* **1992**, *86*, 115.
- Kawatoh, H.; Kakimoto, M.; Tanioka, A. *J. Macromolecules* **1988**, *21*, 625.